

# Stratigraphy, sedimentology and palaeoecology of the dinosaur-bearing Cretaceous strata at Dashuiguo (Inner Mongolia, People's Republic China)<sup>1</sup>.

By Jimmy VAN ITTERBEECK, Pierre BULTYNCK, Guo Wen LI & Noel VANDENBERGHE

VAN ITTERBEECK, J., BULTYNCK, P., LI G. W. & VANDENBERGHE, N., 2001 - Stratigraphy, sedimentology and palaeoecology of the dinosaur-bearing Cretaceous strata at Dashuiguo (Inner Mongolia, People's Republic China). *Bulletin de l'Institut royal des Sciences naturelles, Sciences de la Terre, Supplément 71* : 51-70, 4 pls., 6 figs., 2 tables; Bruxelles-Brussel, December 15, 2001. – ISSN 0374-6291.

## Abstract

The stratigraphy and the sedimentology of the Cretaceous continental dinosaur-bearing strata of the Dashuiguo area have been investigated. A 100 m thick local lithostratigraphic column has been established. It consists of several fining upwards sequences composed of nine lithofacies representing the different sedimentary environments within an alluvial plain. The dinosaur bones are accumulated in bone beds that form the basal lag within the fossil channels (lithofacies Ss). Numerous isolated bones have been retrieved from the cross-bedded sandy infill of those channels. The fossil alluvial river has its source within the nearby Hanwulan Shan that are the source of the sediment load in this river. Based on charophyten evidence the sediments have been attributed to the upper Lower Cretaceous (Barremian-Albian). The paleoclimate is described as a subhumid climate with seasonal dry periods considering the soil type, the fossil fauna and flora and the presence of satin spar veins and evaporitic crystals.

**Key-words:** Sedimentology, Stratigraphy, Cretaceous dinosaur-bearing strata, China, charophytes.

## Résumé

La stratigraphie et sédimentologie des dépôts continentaux à dinosaures qui affleurent dans la région de Dashuiguo ont été étudiées. Une colonne stratigraphique locale d'une épaisseur de 100 m a été établie. Elle est construite de plusieurs séquences positives composées de neuf lithofacies. Ces facies représentent différents environnements sédimentaires dans une plaine alluviale. La rivière alluviale fossile jaillit dans la chaîne de montagnes, Hanwulan Shan. Cette chaîne est la région originelle des sédiments transportés par la rivière. Basés sur les charophytes retrouvés, les couches sont datées comme Crétacé inférieur tardif (Barremien-Albien). Tenant compte du type de sol, la faune et flore fossile et la présence des cristaux d'évaporite et des veines « satin spar », le paléoclimat est décrit comme un climat subhumide avec des périodes sèches.

**Mots-clefs:** Sédimentologie, stratigraphie, dépôts à dinosaures, Crétacé, Chine, charophytes.

## Introduction

Dashuiguo is the ephemeral river with numerous Cretaceous outcrops on its banks near the tiny village of Hanwulan, in the southwestern part of the Inner Mongolia autonomous region (Fig. 1). It is situated 75 km west of the Yellow River and 60 km north of Jilantai (= Jartai), an

industrial town known for its salt production. A Sino-Soviet palaeontological expedition (CHOW & ROZHDESTVENSKY, 1960) discovered dinosaur bones in equivalent strata at the Moartu locality, situated in the vicinity of the studied area. The dinosaur species *Probactrosaurus gobiensis* and *P. alashanicus* have been described from this locality (ROZHDESTVENSKY, 1966). Based on the phylogenetic position of the described dinosaurs an Aptian-Albian age was proposed for the strata (ROZHDESTVENSKY, 1966; NORMAN & WEISHAMPEL, 1990). The Dashuiguo section was investigated by the Sino-Belgian expedition during the summer of 1997 and 1999. A large bone bed with *Probactrosaurus* material was discovered and excavated. The structure and lithology of the area bordering the Dashuiguo River have been mapped and the stratigraphy and the sedimentology were studied. It is the first such study for this region. The primary goals of this study are the stratigraphic positioning of the fossiliferous beds within the local stratigraphic column, a more precise age assignment within the Cretaceous and the characterization of the palaeo-environment.

## General geological setting

The basin where the studied Cretaceous sediments were deposited, is situated between the Lang Shan and the Helan Shan mountain ranges (Fig.1). The first forms together with the Yin Shan mountain range the southern border of the Gobi Basin (JERZYKIEWICZ & RUSSELL, 1991). The last forms the western border of the Ordos Basin (YANG *et al.*, 1986).

According to YANG *et al.* (1986) China can be subdivided into three parts after the Indosinian movement: the Neocathaysian belt in East China, Northwest China and the Qinhai-Xizang plateau (Fig. 2). The studied area is situated in Northwest China near the border (= Helan Shan) with the Neocathaysian belt. The latter is divided in three belts: a western belt characterized by large inland basins (a.o. the Ordos Basin), a central belt characterized by onshore basins and an eastern one with large-scale volcanic activity. These belts were induced by the sub-

1) This paper is a contribution to the Excavation Project BL/36/C12 financially supported by the Federal Office for Scientific, Technical and Cultural Affairs (SSTC-DWTC). J. Van Itterbeeck is aspirant FWO-Vlaanderen.

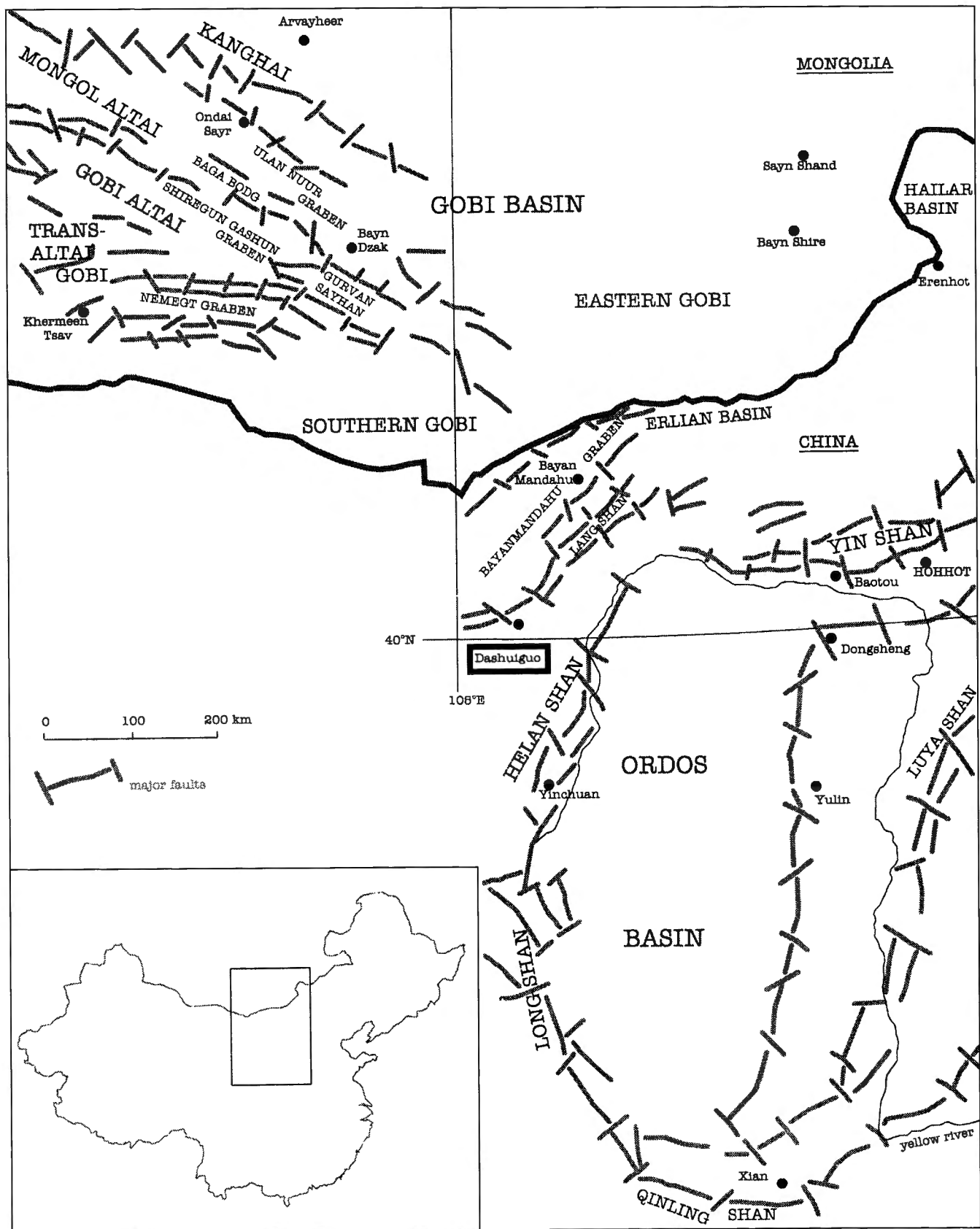


Fig. 1 — Generalized map showing the location of the studied site within the Gobi and Ordos Basin area, inset shows the general location of the area (modified after JERZYKIEWICZ, (1995)).

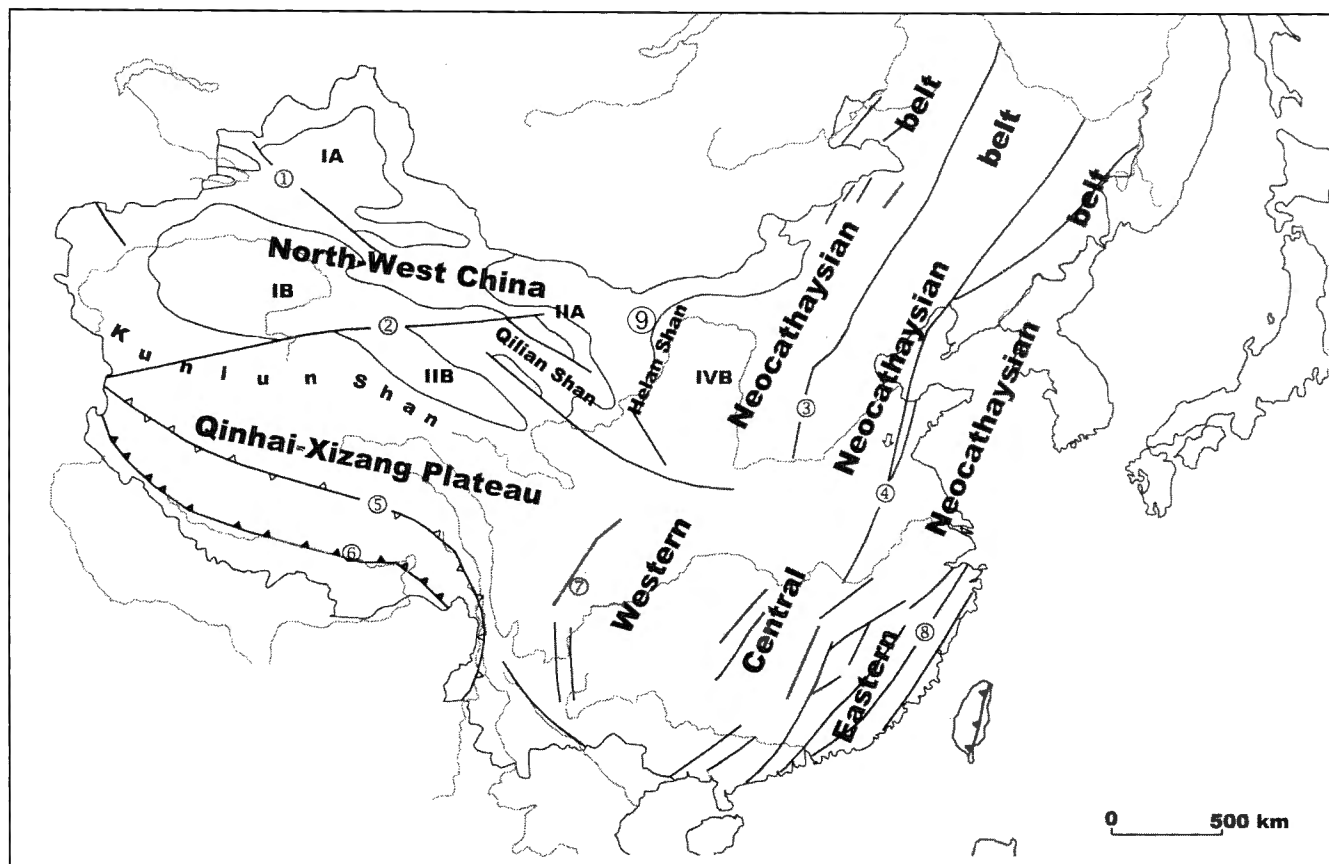


Fig. 2 — Paleotectonic map of China during the post-Indosinian (Yanshanian and Himalayan) stages (modified after YANG *et al.*, (1986)).

I, Tarim Tianshan terrain: IA, Junggar Basin; IB, Tarim Basin. II, Kunlun-Qilian terrain: IIA, Corridor piedmont basins; IIB, Qaidam Basin. IVB, Ordos-Shaanxi Basin  
 Depth faults and crustal consumption zones: ①, North Tianshan; ②, Altyn; ③, Xigana-Taihang; ④, Tancheng-Lujiang; ⑤, Bangong-Nujiang; ⑥, Yarlung Zangbo; ⑦, Longmen; ⑧, Lishui-Haifeng, ⑨ Dashuiguo area.

duction of the Pacific plate underneath the Eurasian continent. Northwest China is bordered by the Helan Shan in the east and by the Kunlun and the Qinling Shan in the south. In this northwestern region alternating big intramontane basins formed by grabens and semigrabens and mountain ranges formed by horst massifs define the structure. They form a basin and range type structure that is the result of the northward movement and collision with the Eurasian continent of the Gondwanan massifs according to YANG *et al.* (1986). An alternative view on the formation of this structure is given by HSU (1989) who believed that the influence of the subduction of the Pacific plate reaches farther inland than the Helan Shan and ascribed the formation of this structure to the regional extension behind an active-plate margin, where the Pacific plate is subducted under the Eurasian continent. The strata at Dashuiguo were deposited in one of the basins forming the basin and range structure of Northwest China with the nearby Hanwulan Shan horst massif, the western prolongation of the Lang Shan as sediment source.

#### Structural outline of the studied area

From the south to the north the outcrops along the Dashuiguo River are divided into three parts based on

their continuity and structural style (Figs. 3 and 4). The folds in the first part, situated opposite the village of Hanwulan, are wide and isoclinal. Their fold axes have a N74E orientation and plunge 5W. No important faults are seen in this part. Monoclinical pendant strata (20-30°W) characterize the second part with a large amount of small faults in the southern part. These faults with displacements ranging from a few centimetres to one meter can easily be recognized in the field as linear features due to the presence of dark red clays along the fault plane. The boundary between the first two parts of the section corresponds to an abrupt change in strike and dip. This line of strike collision indicates the fracture plane but does not allow to estimate the displacement along the fault or to specify its nature. In spite of this tectonic contact characteristic beds recognized on both sides of the fault allow a correlation between part one and two.

The wide and isoclinal folds in the third part have fold axes with a N68W orientation and a plunge of 25E. Numerous faults occur within this part, mostly with small displacements. The end of this part is marked by a dome structure (Pl. 1, Fig. 1). Other remarkable features are a deformed zone at the beginning of this part (Pl. 1, Fig. 3) and the inverted normal fault near the end with an associated bookshelf structure (Pl. 1, Fig. 2). Between the second and the third part only a small number of outcrops

with fractured rocks occur. Their nature or importance could not be assessed. The correlation between these two parts is based on lithological and palaeontological arguments.

**Stratigraphy**

Due to the larger relief and the incision of the river the Quaternary deposits, previously covering the Cretaceous strata, disappeared creating an isolated zone with outcrops. The sediments belong to the Dashuiguo Formation (BUREAU OF GEOLOGY AND MINERAL RESOURCES OF THE NEI MONGOL AUTONOMOUS REGION, 1991). The lower part is described as greyish red conglomerates and sandstones-conglomerates and the upper part consist of brownish-red sandstones, mudstones and black-black mudstones and marls. The estimated thickness of this formation ranges from 228 m to 1449 m. This formation should not be confused with the Dashiguo Formation reported in the literature (YANG *et al.*, 1986). In spite of the small difference in name, this formation occurs in a different region, eastern Gansu and is much older, Middle Jurassic in age. According to our mapping the succession in the Dashuiguo area is about 100 m thick. No contacts

with Cretaceous or Tertiary formations were recognized. It is very likely that not the entire formation is exposed explaining the reduced thickness of the succession. Based on the charophytan evidence the Dashuiguo formation can be correlated with the Jingchuang Formation of the Zhidan group of the Ordos Basin (LI, 1988; LIU, 1999). This formation can be correlated with the Dushilin and Khulsyngol Formations of the Gobi Basin (JERZYKIEWICZ, 1995; JERZYKIEWICZ & RUSSELL, 1991).

**Sedimentary geology**

All sediments of the succession have common characteristics. All sediment grains are angular regardless of their size and most of the strata are micaceous. Both characteristics indicate a nearby source area for the detrital particles, most likely the Hanwulan Shan, a nearby mountain range built up of metamorphic rock. On the geological map these rocks are described as migmatitic gneiss containing andalusite and garnet, granulite, leucogranulite, quartzite with marble and graphite, plagio-amphibolite and quartzite rich in magnetite. The metamorphic rock fragments and the heavy minerals retrieved from the sedi-

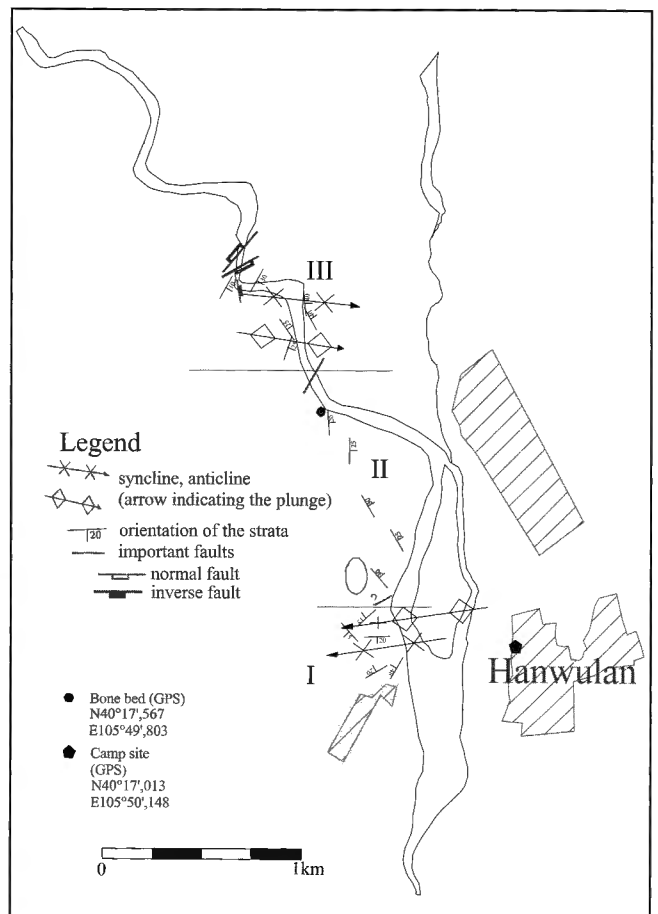
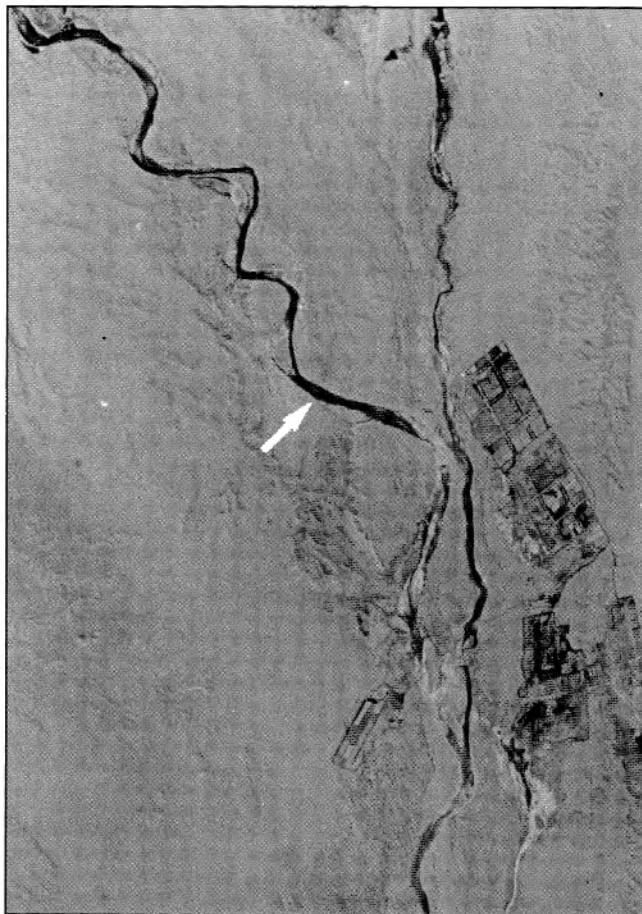


Fig. 3 — Enlargement of satellite image (US Geological Service, Corona satellite image, 1970, DS1110-1006DF001) of the studied area. The arrow indicates the location of the major excavation site.

Fig. 4 — Map of the studied area based on the satellite image (DS1110-1006DF001) with the geological structure and the location of the different outcrops. The outcrops are divided in three parts (Roman numerals). In each part the outcrops are continuous. Between different parts outcrops are lacking or of a poor quality.

ments confirm this hypothesis. In order of decreasing frequency the heavy minerals were identified as magnetite, garnet, andalusite, rutile, tourmaline and epidote. The uplift of the Hanwulan Shan, mainly consisting of Archaean metamorphic rocks, coincided with the development of the sedimentary basin as the basin and range type-structure developed (YANG *et al.*, 1986).

Four lithosomes divided into nine lithofacies were recognized in the Dashuiguo area. The division of the strata into lithofacies and their interpretation is based on MIALL (1996). Wherever it was needed further subdivisions were made applicable to this specific area.

#### Pebbly sands and conglomerates

This lowermost lithosome forms the base of the sedimentary cycles. It is divided in two equivalent lithofacies that never occur together in the same cycle. The two lithofacies are both poorly sorted, coarse-grained deposits containing abundant intraclasts (red silt pebbles) and other lag materials (dinosaur bones, rock fragments).

1. The first lithofacies (Pl. 1, Fig. 4) consists of white coloured, clast-supported, normally graded conglomerate with horizontal stratification (Gh). It consists of angular metamorphic rock fragments (extraclasts) and reworked red coloured silt pebbles (intraclasts). The latter indicate the erosional character of this lithofacies. The bladed to disk shaped silt pebbles have a long axis of 50 cm and a height of 20 cm. They are restricted to the basal part of the facies where the other pebbles obtain a diameter of 20 cm. In the upper part the pebbles have an average dia-

meter of a few centimetres. Within these deposits isolated bone fragments are found. Their preservation is rather bad. The facies attains a thickness of 1-2 m. Besides the horizontal lamination no structures were recognized within this facies. The facies is interpreted as the basal infill of fossil channels.

2. The second lithofacies forms the base of incised channels (Pl. 1, Figs. 6,7; Pl. 2, Fig. 7) and consists of massive coarse pebbly sand (Ss). These pebbles are also angular metamorphic rock fragments and reworked silt pebbles. The facies yields numerous dinosaur bones grouped in bone beds. Associated with the dinosaur bones two bivalve taxa and an occasional fish scale were found. The excavation work during the Sino-Belgian dinosaur expedition was focused on one of these fossil accumulations, which covered an area of approximately 65 m<sup>2</sup>. The bones are white coloured and well preserved despite the transport which they underwent. Due to a diagenetic calcite cementation these deposits are rather indurated hindering the excavation of fossils. A more detailed description of the bone bed will be given with the publication on the study of the dinosaur bones. The thickness of the facies within the succession amounts to 20 cm. The facies is interpreted as a scour fill of the incised channels.

#### Cross-bedded sands

This second lithosome comprises two sandy lithofacies characterized by their cross stratification. Some isolated dinosaur bones were retrieved from these deposits. The sedimentary grains are angular and do not have a frosted

Lithosome	nr	Lithofacies (MIALL, 1996)	Characteristics	Interpretation	Genetic class
In situ carbonates	9	P1	Calcareous nodules, white, root traces	Calcrete	Paleosol facies
	8	P2	Green calcareous beds, presence of Bacteria, Microcodium	Lithified paleosol horizon	
Fossiliferous green marls	7	Fm2	Massive green marl, turtle bones, fish scales, fish teeth, bivalves, gastropods, charophytes, dasycladaceans, ostracods	Abandoned channel	Lacustrine facies
Fine grained sediments	6	Fm1	Fine sands, silts and mud, red, brown, 3 types of bioturbation	Overbank fines	Floodplain facies
	5	F1	Fine sands, silts and mud, fine laminations, white, gray, red, black in color, palynomorphs in black laminae	Overbank fines	
Structured sands	4	Sp	Sand, white or yellow, planar cross beds, isolated bones	Channel infill: 2D-dunes	Channel facies
	3	St	Sand, white or yellow, through cross beds, isolated bones	Channel infill: 3D-dunes	
Pebbly sands and conglomerates	2	Ss	Sand, white, concentration of well preserved bones, presence of pebbles	Scour infill	
	1	Gh	Gravel, white, horizontal laminations, red silt pebbles, eroded bones	Basal infill of channels	

Table 1 — Overview of the different lithofacies recognized in the Lower Cretaceous strata in the Dashuiguo area.

surface. The granulometry of the sediments reveals a population within the coarse sand class and a lack of pronounced sorting. The sets of cross stratification reach a maximum height of 20 cm. Based on the combination of the arguments cited above, the cross-bedded sands at Dashuiguo are considered as non-eolian in origin.

3. The third facies (Pl. 2, Fig. 6) is the dominant sandy facies within the outcrops. It consists of trough cross-bedded medium to coarse-grained sands (St) deposited on top of the above-described facies. Several reactivation and erosional surfaces are recognized within the facies. These bounding surfaces are obvious by the concentration of red silt pebbles or a granulometric break within the sands. The strata are interpreted as sinuous-crested and linguoid subaqueous dunes (3D-dunes) (ASHLEY, 1990). The thickness of these strata amounts to 2-5 m.

4. The fourth lithofacies (Pl. 1, Fig. 5) is an equivalent of the third however distinguished by the planar cross-bedded medium grained sands (Sp). The colour of these sands varies from greyish white to dark yellowish orange (10YR6/6). The yellow sands are confined to the second and third part of the outcrops. Compared to the bedforms of the third facies they indicate a lower flow velocity during deposition. The facies is interpreted as a straight-crested or a transverse subaqueous dune (2D-dunes). The thickness varies from 0.5 to 1 m.

#### Fine grained reddish sediments

5. The fifth lithofacies comprises fine-grained clastics with fine laminations (F1). The granulometry varies from fine sand over silt to mud. The dominant colour is red although white, grey, brown and black coloured laminae also occur. The sediments are interpreted as overbank deposits, laid down during flooding of the alluvial plain. On some occasions gypsum crystals were recognized. The black coloured laminae (Pl. 1, Fig. 2) yield numerous palynomorphs and plant microfossils, which are not discussed in the present paper. Red coloured sediments border the black sediments. This colour transition reflects a change in redox conditions probably due to a change in water table. Within this facies numerous convolute laminations (Pl. 2, Fig. 1) were recognized ranging from simple load casts (Pl. 2, Fig. 2) to more complex forms (Pl. 2, Fig. 3). Similar features are known from the Nemegt Formation in Mongolia (GRADZINSKI, 1969). The generation of these structures is related to a post-depositional upward movement of sediment or pore fluids and air trapped within them. Three mechanisms are known to create these structures: upward vortex induced by turbulent cells on the water (CHAKRABARTI, 1977), sudden impact of loading through bank collapse (CHAKRABARTI, 1977) and sudden impact of loading through passing dinosaurs, dinoturbation. The last can account for the formation of these structures under normal, dry conditions of the floodplain. Under the weight of passing dinosaurs, the sediments on the floodplain can deform leaving dinosaur trackways on the upper surface and deformations within the sediment. The first two mechanisms occur during floods. On top of the deformed strata 10 cm thick layers of pebbly sands (Ss) occur. At their base small erosional scours are visible (Pl. 2, Fig. 4). Within these pebbly sands reworked carbonate nodules and silt pebbles occur. These coarse intercalations are interpreted as crevasse splay deposits (PLATT & KELLER, 1992) formed during

flooding of the alluvial plain. During the flood, bank stability decreases with possible bank collapse and turbulent cells forming in the water mass. This combination of factors leads to the formation of the observed convolute laminations within the overbank fines.

6. Red (10R3/4) and brown (10YR5/4) massive silts and fine sands (Fm1) make up the sixth lithofacies. Within these layers different types of bioturbations were recognized. A first type (Pl. 2, Fig. 8) consists of 10 cm long vertical tubes filled with white calcareous material. The tubes show no branching. They have a round diameter of 0.5 cm. Narrow straight tubes, both horizontal and vertical with black organic material characterize a second type. The diameter is limited to a few millimetres. No branching has been observed within this type. So far neither pollen nor spores have been retrieved from these strata in spite of several analyses and the apparent presence of organic material. A third type of bioturbation (Pl. 2, Fig. 5) consists of red coloured tubes of 10-15 cm with a varying diameter (2-5 cm). The horizontal tubes are unbranched but cross each other. They show longitudinal lines and transverse sections. Within these fine strata one nearly complete skeleton of a small theropod was found. The strata of the sixth lithofacies are interpreted as flood plain sediments equivalent to the laminated fine clastics of the fifth lithofacies. Due to the bioturbation the laminations were not preserved. The deposits attain a thickness of 1 m.

#### Green fossiliferous marl

7. The seventh lithofacies consists of green (5GY6/1) marls (Fm2) with an extremely rich fossil fauna and flora. The facies is several meters thick. The fossil content of these strata consists of dasycladaceans, charophytes, ostracods, bivalves, gastropods, fish scales, fish teeth, turtle bones and eggshell fragments. In this publication only charophytes are studied. Although black spots were recognized, no pollen or spores were obtained from these strata. Charophytes only thrive in still waters or in running waters with only a slight movement (CORILLION, 1975; TAPPAN, 1980). Therefore the facies is interpreted as a lacustrine environment, more probably ponds that formed in abandoned channels in the alluvial plain.

#### In situ carbonates

8. The top of the recognized sequences is characterized by the presence of white calcareous nodules (P1) (Pl. 1, Figs. 3,4). Sometimes the nodules coalesce into continuous beds. In thin section the nodules exhibit a complexly cracked micritic matrix with light and dark grey patches (Pl. 3, Fig. 1). Within the matrix yellow to brown fibrous organic material of plant origin is recognized. The cracks are filled with blocky sparite. Within the nodules rhizoliths (KLAPPA, 1980) were recognized (Pl. 3, Figs. 2,3). They

→  
Fig. 5 — Lithostratigraphic column of the outcropping strata in the Dashuiguo area. The Roman numerals under the columns refer to the different outcrop zones (Fig. 4). The relative height of the different columns reflects the correlation between the columns taken in different parts of the area. The codes mentioned in the legend (Gh, Ss, ...) are the lithofacies codes given in Table I.



show an alveolar-septal texture typical of rhizoliths (WRIGHT *et al.*, 1988) and characteristic of a paleosol (RESTALLACK, 1990). Other non-diagnostic pedogenic features that were recognized are glaebules (= nodules), peds and calcitic cutans surrounding the peds and the sediment grains present within the nodules (Pl. 3, Fig. 4). Associated with these nodules antitaxial veins (Pl. 3, Figs. 5,6) composed of conical outward growing calcite crystals occur in the surrounding sediment (Fm). These satin spar veins (GUSTAVSON *et al.*, 1994) may have originated from dissolution of evaporites within the sediment in infiltrating meteoric water. As a consequence of this dissolution a non-stable cavernous porosity develops, leading to the failure of the sediment and the forming of extensional faults in the overlying rock column. With further dissolution of the evaporites, the groundwater becomes saturated with gypsum. Finally dissolution leads to supersaturation and precipitation of gypsum in the newly formed fractures. Due to diagenesis the gypsum was transformed to calcite. The satin spar veins described by GUSTAVSON *et al.*, (1994) are large-scale phenomena in evaporitic basins whereas the veins found at Dashuiguo are only a few centimeters long and maximum 1 cm thick. Also no continuous evaporitic layers occur, only isolated crystals within the fine-grained strata. Further research is needed to confirm the proposed hypothesis of formation of the calcitic veins found in the Dashuiguo area.

9. Associated with the above-described facies some lithified green calcareous beds (P2) of 10-20 cm thick occur. In thin section the beds can be separated in two types. The first type (Pl. 3, Fig. 7) is characterized by a poikilotopic texture with large angular sparitic crystals. They have a brown colour due to the presence of organic material. After etching with a weak acid ellipsoidal remains of bacteria have been recognized under the electron microscope. There is no doubt on the fossil nature of these bacteria because of their enclosure in the rock and their resistance to electron rays of high intensity. The second type (Pl. 3, Fig. 8) has a radial texture typical for *Microcodium* (KLAPPA, 1978). These textures can be seen more clearly under the electron microscope. Bacteria occur within soils, both recent and fossil (RESTALLACK, 1990). Their association with the calcareous nodules confirms the interpretation of these layers as soil horizons. The presence of *Microcodium* is characteristic of paleosols (KLAPPA, 1978). These soil horizons are lithified due to biological activity.

### Facies assemblages and Architecture

The stratigraphic column is made up of a repetition of the described lithosomes, arranged in cycles. The lithosomes occur in a precise sequence within a cycle. Not all cycles are complete. The general plan of an ideal cycle will be discussed on the basis of a complete cycle recognized within part II of the Dashuiguo area (Fig. 6). The cycle has an erosional base that is represented by an undulating contact with the underlying layer and by reworked intra-clasts. On two occasions a channel was recognized within the outcrop (Fig. 5). At the base of the cycle, the infill of the incision consists of pebbly sands (Ss) although conglomerates are recognized occasionally as a lateral variant. On top of these deposits cross-bedded sands were

laid down (Sp, St). There is a predominance of trough shaped cross beds over planar shaped ones considering the entire stratigraphic column. The rest of the sequence is dominated by fine-grained clastics belonging to the floodplain facies. These deposits can be divided into two types F1 and Fm1, based on the presence of bioturbations and the preservation of the original lamination. These sediments have a dominant reddish colour. Within the overbank fines also coarse intercalations with erosive bases (Pl. 2, Fig. 4) can be found, interpreted as crevasse splay deposits. They were deposited during floods that induced the formation of the convolute laminations (Pl. 2, Figs. 1,2,3). As a laterally equivalent of these fine facies green fossiliferous marls (Fm2) are recognized in some cycles interpreted as a lacustrine facies formed in abandoned channel ponds. Within the overbank fines calcareous paleosols (P1, P2) develop. These calcisols (MACK *et al.*, 1993) are most developed on top of the Fm2 facies where the nodules coalesce into continuous thick banks.

### Depositional environment and climate

The above-described sequences define the depositional environment as an alluvial river, a river running within its sediments. A classification for fossil fluvial systems based on mean grain size of the load, sinuosity and braiding index has been established by MIALL (1985; 1996). However, some of the chosen diagnostic features are difficult to observe in fossil deposits and others are not very diagnostic for particular river types (BRIDGE, 1993). In

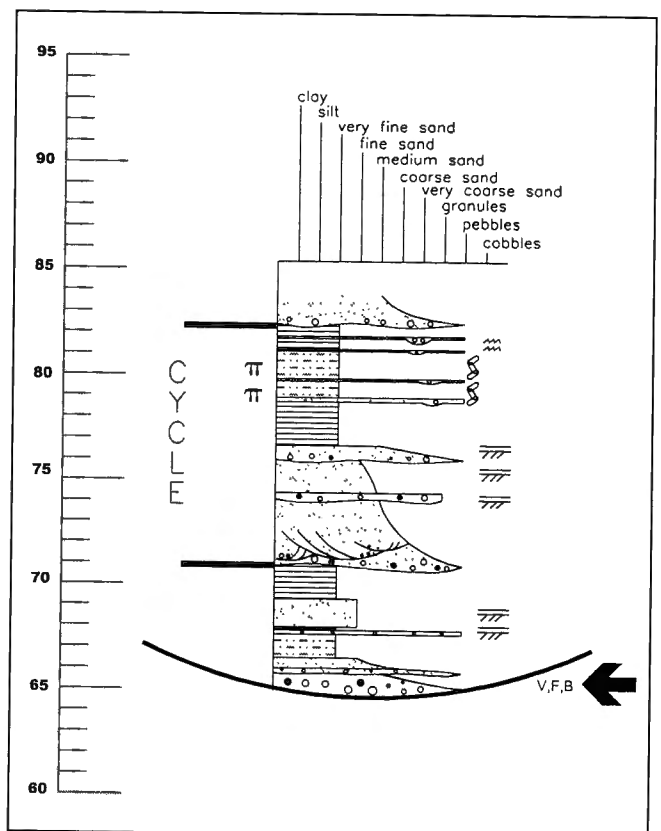


Fig. 6 — Most complete cycle seen within the lithostratigraphic column, enlargement of part of Fig. 5

addition, the tectonic disturbance and the relatively small outcrop area of the studied sediments hinder the application of the proposed classification on the studied strata. Within the studied strata overbank fines form a relatively important part of the succession. Crevasse splay deposits and ponds formed in abandoned channels were recognized. On one occasion an asymmetrical channel with lateral accretion surfaces (Pl. 1, Fig. 8) has been observed. They show great resemblance with the structures known from a point bar deposit.

The calcisols are presently known as well drained soils of semiarid to subhumid regions (RESTALLACK, 1990) supporting vegetation types ranging from desertic scrub to open grassland or grassy woodland with abundant soil fauna. The climatic conditions under which this type of soils occurs allow wetting of the surface layer with leaching of exchangeable cations. In the subsurface the available water volume diminishes due to evaporation, biological activity or absorption by clays leading to the precipitation of  $\text{Ca}^{2+}$  in the Bk-horizon. The depth of this horizon marks the zone of average wetting and allows an estimation of the amount of precipitation for recent soils of this type. In fossil soils the depth of this horizon is difficult to evaluate correctly because of the compaction of the sediments and the possible erosion of the soil above the resistant calcic horizon. Considering the saline nature of the pond water, the presence of evaporite crystals and satin spar veins, a dry climate seems a reasonable hypothesis. The rich herbivorous dinosaur fauna, however, requires a certain amount of vegetation to feed upon, the presence of which is confirmed by the pollen and spores retrieved from the sediments. The rich aquatic fauna and flora found within the Fm2-facies implicate the presence of water within the abandoned channel. Due to evaporation this water has a slightly elevated salinity that prohibits the growth of Clavatoraceae but allows the bloom of the other organisms that were found. Moreover no continuous evaporitic layers have been recognized within the succession, only isolated evaporite crystals occur. The absence of eolian sediments also contradicts a semi-arid climate with restricted vegetation. Therefore a subhumid climate with the development of calcretes under rich vegetation is a more likely hypothesis. The evaporite crystals were formed during seasonally dry periods, which can also account for the evaporation of the pond waters leading to an increase in salinity.

### Systematic Palaeontology

The fossil charophyte floras were recovered from the Fm2-lithofacies. Besides charophytes this facies also contains ostracods and microvertebrates which will be described later.

Order Charales LINDLEY, 1836  
Family Porocharaceae GRAMBAST, 1962  
Genus *Porochara* MÄDLER, 1955

*Porochara mundula* (PECK) SHAJKIN  
Plate 4, Fig. 1

1941 *Aclistochara mundula* (PECK), n.sp. - PECK, p.291, pl.42, fig.7-11.

- 1957 *Stellatochara mundula* (PECK) - PECK, p.29, pl. 3, fig.25-35.
- 1976 *Porochara mundula* (PECK) - SHAJKIN, p.80.
- 1976 *Euaclistochara mundula* (PECK), n. comb. - Z. WANG *et al.*, p.71.
- 1978 *Porochara? mundula* (PECK) L. GRAMBAST -Z. WANG, p.71, pl.2, fig.17-26.

### MATERIAL

More than 100 well preserved specimens often with internal calcite crystallisation.

### DESCRIPTION

Small subovoid, prolate to subprolate gyrogonites with a conspicuously truncated summit and a broadly rounded base. Large apical pore occupying the entire summit area. Pore circular to pentagonal in shape with cellular spirals forming a rosette around the pore. Five sinistral cellular spirals with sharp and narrow intercellular ridges.

Measurements of 50 specimens: length, maximum 460  $\mu\text{m}$ , minimum 340  $\mu\text{m}$ , average 416  $\mu\text{m}$ ; width, maximum 340  $\mu\text{m}$ , minimum 260  $\mu\text{m}$ , average 307  $\mu\text{m}$ ; ISI (= Isopolarity Index), maximum 192, minimum 120, average 136; diameter of apical pore, maximum 120  $\mu\text{m}$ , minimum 80  $\mu\text{m}$ , average 96  $\mu\text{m}$ ; 3 specimens with 8 spiral ridges in side view, 17 with 9 ridges, 27 with 10 ridges and 2 with 11 ridges.

### AFFINITIES AND DIFFERENCES

*Porochara mundula* has been attributed to different genera. It does not belong to the genus *Aclistochara* because it has an apical pore, nor to *Stellatochara* because of the different summit structure. *Euaclistochara* is an invalid genus (LU, 1997) and a synonym for *Porochara* (FEIST & GRAMBAST-FESSARD, 1982). The characteristic shape with the truncated summit and the large apical pore make this species easy to identify.

### OCCURRENCE

*Porochara mundula* is abundant in the Aptian and Albian sediments of the Rocky Mountains, US (PECK, 1941; PECK, 1957), in the Lower Cretaceous of Chubut and Neuquen provinces, Argentina (MUSACCHIO, 1972; MUSACCHIO & CHELBI, 1975), in the Upper Daegu and Lower Geonchunri (Lower Cretaceous) Formations, Korea (CHOI, 1987), In China it is commonly known from the upper Lower Cretaceous to the lower Upper Cretaceous, e.g. the upper part of the upper member of the Jingchuan Formation (Albian) of the Ordos Basin (LI, 1988), the Honglishan and Hongshaquan Formations of the Junggar Basin (LIU & WU, 1990), the Lower Cretaceous of the Hetao Basin, Inner Mongolia (SHU & ZHANG, 1985), the third and fourth member of the Quantou Formation (Aptian-Albian) of the Songliao Basin (Z. WANG *et al.*, 1985), the Miaoshanhu and Bayanhot Formation (Upper Barremian) of the Bayanhot Basin (LU & YUAN, 1991), the Jidian assemblage (Aptian) of the Yangtze-han river Basin (Z. WANG, 1978), the Shushanhe and Baxigai Formations of the Tarim Basin, Xinjiang (LU & LUO, 1990) and the Wujiashan section (Aptian-Campanian) in Tianzhen, Shanxi and Yuangyuan, Hebei (LIU & PANG, 1999) and the Nemegt Formation (Lower Campanian) of Mongolia (KARCZEWSKA & ZIEMBIŃSKA-TWORDZYDŁO, 1983).

STRATIGRAPHICAL RANGE  
Barremian to Campanian

Genus *Minhechara* WEI, HAO *et al.*, 1983

*Minhechara xiaoxiaensis* YANG & ZHOU, 1983  
Plate 4, Fig. 3

- 1983 *Minhechara xiaoxiaensis* gen. et sp. nov. YANG  
et ZHOU -HAO *et al.*, p.174, pl. 43, fig.7-10.  
1990 *Latochara xiaoxiaensis* -LU & LUO, p.62, pl.6,  
fig.5, 6.

MATERIAL  
2 well preserved gyrogonites

DESCRIPTION  
Spherical gyrogonites with rounded base and apex. No change in thickness and width of cellular spirals near the apex. Spiral cells vertical in the apical centre forming a prominent apical structure with a small apical pore. Spirals cells thickened at base forming a cage surrounding the basal opening.  
Measurements of two specimens: Specimen 1, length 350 µm, width 300 µm, ISI 117, 11 spiral ridges in side view; Specimen 2, length 320 µm, width 300 µm, ISI 107, 9 spiral ridges in side view.

AFFINITIES AND DIFFERENCES  
According to FEIST & GRAMBAST-FESSARD (1991) the genus *Minhechara* is an invalid synonym for *Latochara*. However in the publication of LU (1997) on the genera named by Chinese authors, *Minhechara* is considered as a valid genus. The studied gyrogonites show the typical pronounced apical structure with a small pore of *Minhechara xiaoxiaensis*. The type species of this genus, *Minhechara columelaria*, has a greater number of spirals in lateral view and the apical structure is less pronounced. The cellular spirals at the base show no nodules and form no basal cage contrary to the studied specimens.

OCCURRENCE  
*Minhechara xiaoxiaensis* is known from the Hekou Formation (Lower Cretaceous) of the Xining and Minhe Basin (HAO *et al.*, 1983), from the Qigu (Upper Jurassic) and the Shushanhe (Berriasian-Barremian) Formations of the Tarim Basin (LU & LUO, 1990) and from the Quanyagou group (Aptian) of the Qaidam Basin (TANG & DI, 1991).

STRATIGRAPHICAL RANGE  
Upper Jurassic-Aptian

Family Characeae AGARDH, 1824  
Genus *Aclistochara* PECK, 1937

*Aclistochara bransoni* PECK, 1937  
Plate 4, Fig. 2

- 1937 *Aclistochara bransoni* PECK, n. sp. - PECK, p.87,  
pl.14, fig.8-11.

- 1937 *Aclistochara lata* PECK, n. sp. - PECK, p.88,  
pl.14, fig.20-23.  
1937 *Aclistochara oligospirata* PECK, n. sp. - PECK,  
pl.14, fig.5-7.  
1937 *Aclistochara elongata* PECK, n. sp. - PECK, pl.  
14, fig.24-25.  
1957 *Aclistochara bransoni* PECK - PECK, p.26, pl.4,  
fig.1-14.  
1965 *Aclistochara huihuibaoensis* sp. nov. - S.WANG,  
p.471,489, pl.II, fig.1.  
1965 *Aclistochara lata* PECK - S.WANG, p.470,488,  
pl.II, fig.7.  
1965 *Aclistochara laiae* sp. nov. - S.WANG,  
p.470,488, pl.VI, fig.6.  
1965 *Aclistochara hungarica* RASKY - S.WANG,  
p.472,490, pl.II, fig.2.  
1965 *Aclistochara sp.* - S.WANG, p.472,490, pl.II,  
fig.3-5.  
1965 *Aclistochara caii* sp. nov. - S.WANG, p.471,489,  
pl.II, fig.8.

MATERIAL  
more than 100 specimens often deformed due to the lack of calcite crystallisation inside.

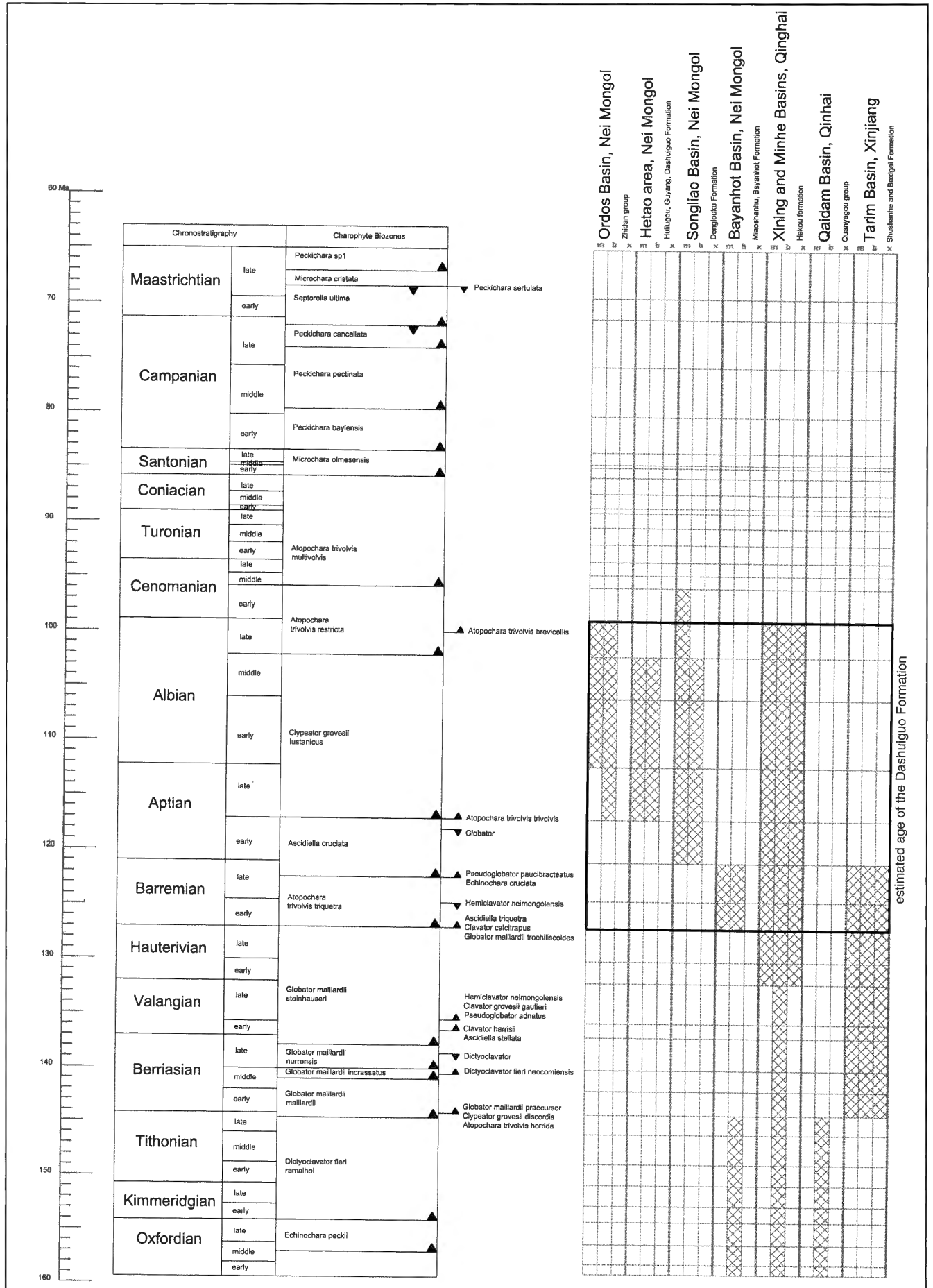
DESCRIPTION  
Small prolate spherical, subovoidal gyrogonites with a rounded base and a deeply truncated summit. Basal plate composed of two elements. Cellular spirals forming a rim around distinct apical depression. Junctions of the cellular spirals in this depression not visible due to sediment cover. Cellular spirals convex with sharp and narrow intercellular ridges.  
Measurements of 50 specimens: length, maximum 500 µm, minimum 340 µm, average 422 µm; width, maximum 440 µm, minimum 320 µm, average 395 µm; ISI, maximum 97, minimum 115, average 107; 14 specimens with 6 spiral ridges in side view, 31 with 7 ridges and 5 with 8 ridges.

AFFINITIES AND DIFFERENCES  
The studied specimens bear a great resemblance to *Aclistochara bransoni* and different *Aclistochara* species described by S. WANG, (1965): *A. laiae*, *A. huihuibaoensis*, *A. caii* and *A. sp.* According to FU & LU, (1997) only *A. huihuibaoensis* is a valid species and the three other species described by S. WANG, (1965) are considered as synonyms. However, in the original description of *A. huihuibaoensis* S.WANG, (1965) mentions that it is impossible to distinguish it from *A. bransoni* as described by PECK, (1957). Therefore *A. huihuibaoensis* is considered herein to be a synonym for *A. bransoni*.

OCCURRENCE  
Originally described from the Morrison Formation (Kimmeridgian-Tithonian) of the US (PECK, 1937; 1957).



Table 2 — Stratigraphic distribution of the charophyte species found in the Dashuiguo area within the neighbouring basins and the positioning of these assemblages within the charophyte biozonation established by RIVELINE *et al.*, (1996) (chronostratigraphy based on HARDENBOL *et al.*, (1998)).



In Europe it is known from the Kimmeridgian to the Valanginian of Northwest Germany (SCHUDACK, 1990), from the Oxfordian of southeastern France and Switzerland (MOJON, 1989). In Asia the species is known from the Kimmeridgian of Mongolia (KYANSEP-ROMASHKINA, 1975) and from the Tithonian of Romania (SHAJKIN, 1976).

In China it is known from the Upper Jurassic to the Lower Cretaceous e.g. the lower part of the lower Huihuibao Formation (base of the Cretaceous) of the Jiuquan Basin, Kansu (S.WANG, 1965), from the Upper Jurassic (Kimmeridgian-Tithonian, assemblage III) of Sichuan Province (LIU, 1982), from the lower Dantonghe Formation (Upper Jurassic to Lower Cretaceous) of the Xining and Minhe Basins, Qinghai (HAO *et al.*, 1983), from the Lower Cretaceous of the Hetao area in Inner Mongolia (SHU & ZHANG, 1985), from the Denglouku Formation (Aptian) of the Songliao Basin, Heilongjiang (Z. WANG *et al.*, 1985), from the Tugulu group (Lower Cretaceous) of the Junggar Basin, Xinjiang (LIU & WU, 1985), from the Qigu Formation (Upper Jurassic) of the Tarim Basin, Xinjiang (LU & LUO, 1990), from the Hongshuigou Formation (Upper Jurassic) of the Qiadam Basin, Qinhai (TANG & DI, 1991), from the Luohangdong (Barremian, Lower Barremian) and Jingchuan (Upper Barremian to Albian, Barremian) Formations of the Zhidan group in the Ordos Basin (LI, 1988; LIU, 1999).

STRATIGRAPHICAL RANGE  
Kimmeridgian-Albian.

### Age

For the age determination of Cretaceous continental deposits by charophytes, Clavatoraceae are used because of their rapid and well-known evolution (GRAMBAST, 1974). For Europe charophyte biozonations mainly based on this group have been established (RIVELINE *et al.*, 1996). The studied flora however contains no members of the Clavatoraceae. Probably the environmental factors were not favourable for these charophytes. The presence of *Porochara mundula* indicates a certain amount of salinity (most favourably 3-5 ‰) in the water (SCHUDACK, 1993), as do the Dasycladaceae (Pl. 4, Fig. 4) that were found together with the charophytes. Considering the distance of the basin to the sea, the elevated salinity is due to the evaporation of the water. This conclusion is confirmed by the presence of the evaporite crystals and satin spar veins (cf supra).

In spite of the lack of clavatoraceans the age of the strata based on charophytes is obtained by comparison with floras that have been placed within the charophyte zonation. The studied flora shows a resemblance to the flora known from the Upper Barremian strata (*Atopochara trivolvis triquetra-Flabellochara hebeiensis* assemblage) from the Bayanhot basin (LU & YUAN, 1991), the Aptian strata (*Atopochara trivolvis trivolvis* zone) from the

Songliao basin (Z. WANG *et al.*, 1985) and from the Hetao area of Inner Mongolia (SHU & ZHANG, 1985).

These assemblages correspond to the *Atopochara trivolvis triquetra* zone (Barremian) and the *Clavator grovesii lusitanicus* zone (Upper Aptian to Middle Albian) (RIVELINE *et al.*, 1996). Therefore the studied flora is attributed to the Barremian-Albian interval.

This estimation perfectly matches the ages of the other formations given in Table 2. The only exception is the age of the Shushanhe formation of the Tarim Basin (LU & LUO, 1990). The lower boundary of the age interval of this formation is based on the presence of *Clypeator zongjiangensis*. The upper boundary is based on the presence of *Porochara mundula* and *Minhechara xiaoxiaensis*. Therefore the age interval of this formation does not contradict our conclusions for the Dashuiguo formation.

### Conclusions

Based on the charophytan evidence, the continental strata in the Dashuiguo area are considered to be Barremian-Albian in age. The same charophytes allow a correlation with the Jingchuang Formation of the Zhidan group of the Ordos Basin (LI, 1988; LIU, 1999) and the Dushilin and Khulsyngol Formations of the Gobi Basin (JERZYKIEWICZ, 1995; JERZYKIEWICZ & RUSSELL, 1991). These formations belong to the Khukhetian "Age" which according to JERZYKIEWICZ & RUSSELL, (1991) ends before the Late Albian, at about 100 Ma.

Based on the sedimentological characteristics, the deposits are considered as ancient river deposits. The sediments were transported from the nearby Hanwulan Shan, their region of provenance. On the floodplain of the ancient river, herbivorous dinosaurs (*Probactrosaurus*) grazed the vegetation that grew in a subhumid climate with occasional dry periods. Rarely articulated remains of dinosaurs were preserved on the floodplain. Bones were mostly transported and reworked by the river and deposited as isolated elements in the cross-bedded facies (St, Sp) or concentrated in bone beds (Ss). By the migration of the river, abandoned channel ponds were created. Within these ponds, the local fauna and flora thrived.

### Acknowledgements

We are grateful to SHAO Qing-Long (Inner Mongolia Museum), Monnik DESMETH (Office of Scientific, Technical and Cultural Affairs) and CHEN Ming (Scientific and Technical Service of the Chinese Embassy in Belgium) for treating the administrative and financial aspects of the second excavation campaign at Dashuiguo. All the Chinese and Belgian participants in the fieldwork at Dashuiguo during the summer of 99 are thanked for their help and company. Monique FEIST gave invaluable assistance for the determination of the charophytes during a study leave of the first author at the university of Montpellier. D.A. EBERTH kindly reviewed the manuscript.

## References

- AGARDH, C.A., 1824. *Systema algarum*, Lund, 312 pp.
- ASHLEY, G.M., 1990. Classification of large-scale subaqueous bedforms: a new look at an old problem. *Journal of Sedimentary Petrology*, **60** (1): 160-172.
- BRIDGE, J.S., 1993. Description and interpretation of fluvial deposits: a critical perspective. *Sedimentology*, **40**: 801-810.
- BUREAU OF GEOLOGY AND MINERAL RESOURCES OF THE NEI MONGOL AUTONOMOUS REGION, 1991. Regional geology of Nei Mongol (Inner Mongolia) autonomous region, People's Republic of China. Geological Publishing House, Beijing, 725 pp. (in Chinese with English summary).
- CHAKRABARTI, A., 1977. Upward Flow and Convolute Laminations. *Senckenbergiana Maritima*, **9** (5/6): 285-305.
- CHOI, S.J., 1987. Study on the Lower Cretaceous Charophytes from the Upper Gyeongsang Supergroup. *Journal of the Paleontological Society Korea*, **3**: 79-92.
- CHOW, M. & ROZHDESTVENSKY, A.K., 1960. Exploration in Inner Mongolia. *Vertebrata Palasiatica*, **IV** (1): 1-10.
- CORILLION, R., 1975. Flore des Charophytes (Characées) du Massif Armoricain et des contrées voisines d'Europe occidentale. Jouve Éditeurs, Paris, 216 pp.
- FEIST, M. & GRAMBAST-FESSARD, N., 1982. Clé de détermination pour les genres de charophytes. *Paléobiologie continentale*, **13**: 1-28.
- FEIST, M. & GRAMBAST-FESSARD, N., 1991. The genus concept in Charophyta: evidence from Palaeozoic to Recent. In: RIDING, R. (Ed.) *Calcareous Algae and Stromatolites*, Proceedings of an International Symposium on Fossil Algae, Cardiff, 1987. Springer Verlag, New York, pp. 189-203.
- FU, J. & LU, H., 1997. Early Cretaceous fossil charophytes from Xiagou formation at Jiedabangou, Huahai basin, Gansu. *Acta Micropalaeontologica Sinica*, **36** (3): 350-357. (in Chinese).
- GRADZINSKI, R., 1969. Sedimentation of dinosaur-bearing Upper Cretaceous deposits of the Nemegt basin, Gobi desert. *Palaeontologia Polonica*, **21**: 148-229.
- GRAMBAST, L., 1962. Classification de l'embranchement des Charophytes. *Naturalia Monspeliensia, Série Botanique*, **14**: 63-86.
- GRAMBAST, L., 1974. Phylogeny of the Charophyta. *Taxon*, **23** (4): 463-481.
- GUSTAVSON, T.C., HOVORKA, S.D. & DUTTON, A.R., 1994. Origin of Satin Spar veins in evaporite basins. *Journal of Sedimentary Petrology*, **A64** (1): 88-94.
- HAO, Y., RUAN, P., ZHOU, X., SONG, Q., YANG, G., CHENG, S. & WEI, Z., 1983. Middle Jurassic-Tertiary deposits and ostracod-charophyta fossil assemblages of Xining and Minhe basins, 179 pp. (in Chinese).
- HARDENBOL, J., THIERRY, J., FARLEY, M.B., JACQUIN, T., DE GRACIANSKY, P.-C. & VAIL, P.R., 1998. Mesozoic and Cenozoic sequence chronostratigraphic framework of the European basins. In: DE GRACIANSKY, P.-C., HARDENBOL, J., JACQUIN, T. & VAIL, P.R. (Eds.) *Mesozoic and Cenozoic sequence stratigraphy of European basins*. SEPM, Tulsa, pp. 3-13.
- HSU, K.J., 1989. Origin of sedimentary basins of China. In: ZHU, X. (Ed.) *Chinese sedimentary basins*. Elsevier, Amsterdam, pp. 207-227.
- JERZYKIEWICZ, T., 1995. Cretaceous vertebrate-bearing strata of the Gobi and Ordos basins - a demise of the Central Asian lacustrine dinosaur habitat. *Proceedings of the 15th international Symposium of Kyungpook National University*: 233-256.
- JERZYKIEWICZ, T. & RUSSELL, D.A., 1991. Late Mesozoic stratigraphy and vertebrates of the Gobi basin. *Cretaceous Research*, **12**: 345-377.
- KARCZEWSKA, J. & ZIEMBINSKA-TWORDZYDLO, M., 1983. Age of the Upper Cretaceous Nemegt Formation (Mongolia) on charophytan evidence. *Acta Palaeontologica Polonica*, **28** (1-2): 137-146.
- KLAPPA, C.F., 1978. Biolithogenesis of Microcodium: elucidation. *Sedimentology*, **25**: 489-522.
- KLAPPA, C.F., 1980. Rhizoliths in terrestrial carbonates: classification, recognition, genesis and significance. *Sedimentology*, **27**: 613-629.
- KYANSEP-ROMASHKINA, N.P., 1975. Nekotorye Pozoneyurskie i Melovye Kharofity Mongolii (Some charophytes from the Upper Jurassic and the Cretaceous of Mongolia). *Iskopaemye Fauna i Flora Mongolii Sovmestnaya Sovetsko-Mongolskaya paleontologicheskaya ekspeditsia Trudy*, **2** (181-204).
- LI, Z., 1988. Fossil charophytes from the Zhidan group from the western border of the Ordos basin. *Acta Micropalaeontologica Sinica*, **5** (3): 283-295. (in Chinese).
- LINDLEY, J., 1836. A natural system of Botany. Longman, Rees, Orme, Brown, Green and Longman, London, 414 pp.
- LIU, J., 1982. Jurassic Charophytes from Sichuan province. *Bulletin of the Institute of Geology, Chinese Academy of Geological Sciences*, **5**: 97-110. (in Chinese).
- LIU, J., 1999. Charophytes from the Early Cretaceous Zhidan group in South-Western Ordos Basin. *Professional Papers of Stratigraphy and Palaeontology*, **17**: 244-249. (in Chinese).
- LIU, J. & PANG, Q., 1999. Charophyte flora from the Late Cretaceous in Tianzhen Shanxi province and Yangyuan, Hebei province. *Professional Papers of Stratigraphy and Palaeontology*, **27**: 1-7. (in Chinese).
- LIU, J. & WU, X., 1985. Charophytes from Tugulu group of the Junggar basin. *Bulletin of the Institute of Geology, Chinese Academy of Geological Sciences*, **11**: 139-153. (in Chinese).
- LIU, J. & WU, X., 1990. Cretaceous Tertiary Charophytes fossil in Northern Xinjiang. In: *The study on the Micropaleobotany from Cretaceous Tertiary of the oil bearing basins in some regions of Qinghai & Xinjiang*. Edition China Environment Science Press, pp. 181-229. (in Chinese).
- LU, H., 1997. On charophyte genera named by Chinese authors. *Acta Micropalaeontologica Sinica*, **14** (4): 391-404.
- LU, H. & LUO, Q., 1990. Fossil Charophytes from the Tarim basin, Xinjiang. Science and Technic Documents, Publishing House, 261 pp. (in Chinese).
- LU, H. & YUAN, K., 1991. Jurassic and Early Cretaceous charophytes from the Bayanhot basin and its neighbourhood. *Acta Micropalaeontologica Sinica*, **8** (4): 373-394. (in Chinese).
- MACK, G.H., JAMES, C.W. & MONGER, C.H., 1993. Classification of paleosols. *Geological Society of America Bulletin*, **105**: 129-136.
- MÄDLER, K., 1955. Die taxonomischen Prinzipien bei der Beurteilung fossilen Charophyten. *Paläontologische Zeitschrift*, **29**: 103-108.
- MIALL, A.D., 1985. Architectural-element analysis: a new method of facies analysis applied to fluvial deposits. *Earth Science Reviews*, **22**: 261-308.
- MIALL, A.D., 1996. *The Geology of Fluvial Deposits: Sedimentary Facies, Basin Analysis and Petroleum Geology*. Springer Verlag, New York, 582 pp.
- MOJON, P.O., 1989. Charophytes et ostracodes laguno-lacustres

- du Jurassique de la Bourgogne (Bathonien) et du Jura septentrional franco-suisse (Oxfordien). Remarques sur les discontinuités émersives du Kimmeridgien du Jura. *Revue de Paléobiologie*, **3** (volume spécial): 1-18.
- MUSACCHIO, E.A., 1972. Carofitas del Cretacico inferior en sedimentitas "Chubutenses" al este de la Herreria, Chubut. *Ameghiniana*, **9** (4): 354-356.
- MUSACCHIO, E.A. & CHELBI, G., 1975. Ostracodos no marinos y Carofitas del Cretacico inferior en las provincias de Chubut y Neuquen, Argentina. *Ameghiniana*, **12** (1): 70-96.
- NORMAN, D.B. & WEISHAMPEL, D.B., 1990. Iguanodontidae and related Ornithomimids. In: WEISHAMPEL, D.B., DODSON, P. & OSMOLSKA, H. (Eds.) *The Dinosauria*. University of California Press, Berkeley, pp. 510-533.
- PECK, R.E., 1937. Morrison Charophyta from Wyoming. *Journal of Paleontology*, **11** (2): 83-90.
- PECK, R.E., 1941. Lower Cretaceous Rocky Mountain nonmarine microfossils. *Journal of Paleontology*, **15** (3): 285-304.
- PECK, R.E., 1957. North American Mesozoic Charophyta. United States Government Printing Office, Washington, 44 pp.
- PLATT, N.H. & KELLER, B., 1992. Distal alluvial deposits in a foreland basin setting - the Lower Freshwater Molasse (Lower Miocene), Switzerland: sedimentology, architecture and paleosols. *Sedimentology*, **39**: 545-565.
- RETAILLACK, G.J., 1990. Soils of the past: an introduction of paleopedology. Unwin Hyman, Boston, 520 pp.
- RIVELINE, J., BERGER, J.-P., FEIST, M., MARTIN-CLOSAS, C., SCHUDACK, M.E. & SOULIÉ-MÄRSCHÉ, I., 1996. European Mesozoic-Cenozoic charophyte biozonation. *Bulletin de la Société Géologique de France*, **167** (3): 453-468.
- ROSHDESTVENSKY, A.K., 1966. New Iguanodonts from Central Asia: phylogenetic and taxonomic relationships between late Iguanodontidae and early Hadrosauridae. *Paleontologicheskii Zhurnal*: 103-116.(in Russian).
- SCHUDACK, M., 1990. Bestandsaufnahme und Lokalisation der Charophyten aus Oberjura und Unterkreide des Nordwestdeutschen Beckens. *Berliner geowissenschaftliche Abhandlungen*, **A 124**: 209-245.
- SCHUDACK, M.E., 1993. Möglichkeiten palökologischer Aussagen mit Hilfe von fossilen Charophyten. In: Festschrift Prof. W. Krutzsch. Museum für Naturkunde, Berlin, pp. 39-60.
- SHAJKIN, I.M., 1976. New data on biostratigraphy of the Jurassic Cretaceous deposits of the Fore-Dobrogean trough. *Geologicheskii Zhurnal Kiev*, **36** (77-86).(in Russian).
- SHU, Z. & ZHANG, Z., 1985. Early Cretaceous charophytes from the Hetao area of Inner Mongolia. *Contributions to the First Fossil Charophyte Symposium of China*: 63-74.(in Chinese).
- TANG, L. & DI, H., 1991. Fossil Charophytes from Qaidam Basin, Qinghai. Scientific and technical Documents Publishing House,, p1-188 pp.(in Chinese).
- TAPPAN, H., 1980. Charophytes and Umbellinaceans. In: *The Paleobiology of Plant Protists*. Freeman & Co, San Francisco, pp. 913-963.
- WANG, S., 1965. Mesozoic and Tertiary Charophyta from Yiuquan basin of Kansu province. *Acta Paleontologica Sinica*, **13** (3): 463-509.(in Chinese).
- WANG, Z., 1978. Cretaceous Charophytes from the Yangtze-Han river basin with a note on the classification of Porocharaceae and Characeae. *Memoirs of Nanjing Institute of Geology and Palaeontology, Academia Sinica*, **9**: 61-88.(in Chinese).
- WANG, Z., HUANG, R. & WANG, S., 1976. Mesozoic and Cenozoic Charophyta from Yunnan Province. In: ACADEMIA SINICA, NANJING GEOLOGICAL AND PALAEOBIOLOGICAL INSTITUTE (Ed.) *Mesozoic fossils of Yunnan*. Science Press, pp. 65-86.(in Chinese).
- WANG, Z., LU, H. & ZHAO, C., 1985. Cretaceous charophytes from Songliao basin and adjacent areas. Tectonic and Scientific Press of Hi Long Jiang, Haerbin, 75 pp.(in Chinese).
- WRIGHT, V.P., PLATT, N.H. & WIMBLETON, W.A., 1988. Biogenic laminar calcretes: evidence of calcified root-mat horizons in paleosols. *Sedimentology*, **35**: 603-620.
- YANG, Z.Y., CHENG, Y. & WANG, H., 1986. The geology of China. Oxford Science, Oxford, 303 pp.

J. Van Itterbeeck (aspirant FWO-Vlaanderen)  
& N. Vandenberghe  
Afdeling Historische Geologie  
Katholieke Universiteit Leuven  
Redingenstraat 16  
B-3000 Leuven  
Belgium

E-mail: jimmy.vanitterbeeck@geo.kuleuven.ac.be

P. Bultynck  
Department of Palaeontology  
Royal Belgian Institute of Natural Sciences  
Vautierstraat 29  
B-1000 Brussel  
Belgium

E-mail: pierre.bultynck@naturalsciences.be

Wen Guo Li  
Zhongghuan Road  
Xincheng District, Huhhot 010010  
Inner Mongolia, P.R. China.

## PLATE 1

- Fig. 1 — Dome structure cropping out at the northern edge of part III.  
 Fig. 2 — Overview of an inverse fault with an associated bookshelf structure on the right positioned in the middle of part III. Black laminated silts (F1) are rich in palynomorphs.  
 Fig. 3 — Deformed zone at the southern border of the third group of outcrops. An estimation of the deformation can be made by following the green-gray calcareous bed (P2) that start left of the person on the picture. In the upper left corner white calcareous nodules (P1) are visible.  
 Fig. 4 — Detail of the Gh facies with the presence of large ellipsoidal red silt pebbles (intraclasts). In the underlying layer white calcareous nodules (P1) stick out against the surrounding red sediment.  
 Fig. 5 — Overview of a channel (white sands) that are incised in the underlying red silts.  
 Fig. 6 — Detail of the Sp facies showing to sets of planar crossbedded strata.  
 Fig. 7 — Detail of the incision in the underlying sediments (1 unit on the graduated ruler = 10cm).  
 Fig. 8 — Detail of the lateral accretion surfaces visible within sandy channel fill in the deepest part of the channel.

## PLATE 2

- Fig. 1 — Overview of an outcrop in part II near the excavated bonebed that consist almost entirely of F1 and Fm1 sediments. Within these laminated fines several types of convolute laminations can be observed. Figures 2 to 4 are more detailed views of the outcrop. The exact position is indicated by arrows and numerals.  
 Fig. 2 — Detail of the loadcasts in the upper right of figure 1.  
 Fig. 3 — Enlargement of the area covered by the hammer on figure 1 showing complex convolute laminations.  
 Fig. 4 — Enlargement of pebbly sand layer covering the load cast structures with erosional scour below the scale bar.  
 Fig. 5 — Type 1 Bioturbation structure.  
 Fig. 6 — Detail of St with several sets of trough cross bedded strata and reactivation surfaces.  
 Fig. 7 — Detail of the channel infill (plate I, Fig.6) showing to pronounced fining upward cycles.  
 Fig. 8 — Type 3 Bioturbation structure, scale bar resting on the bedding plane.

## PLATE 3

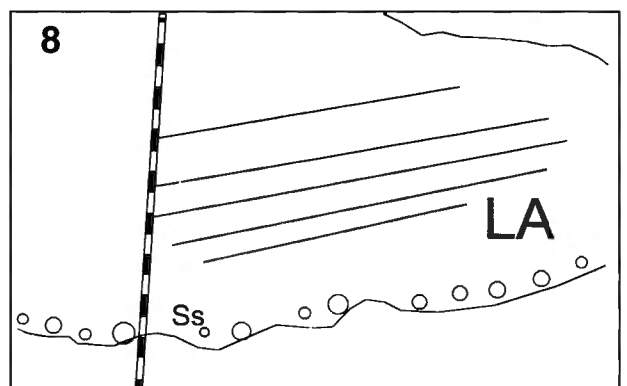
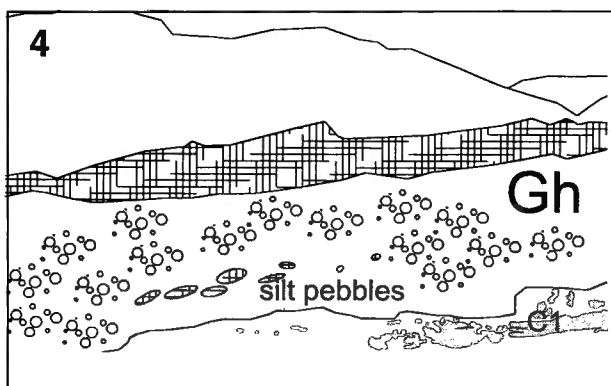
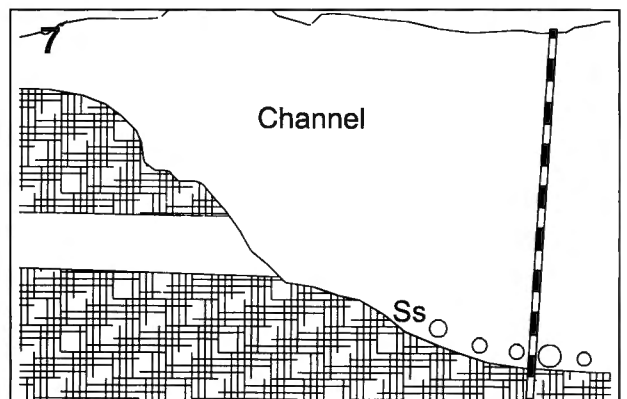
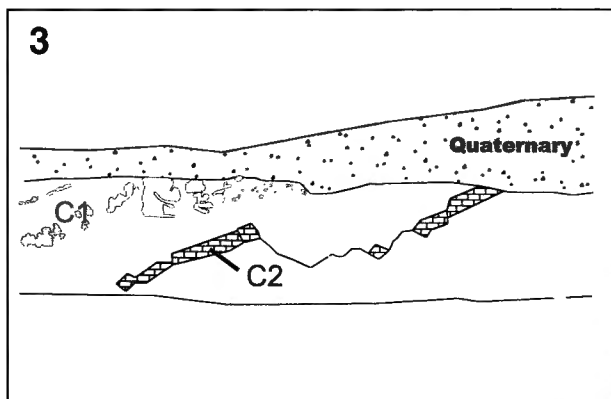
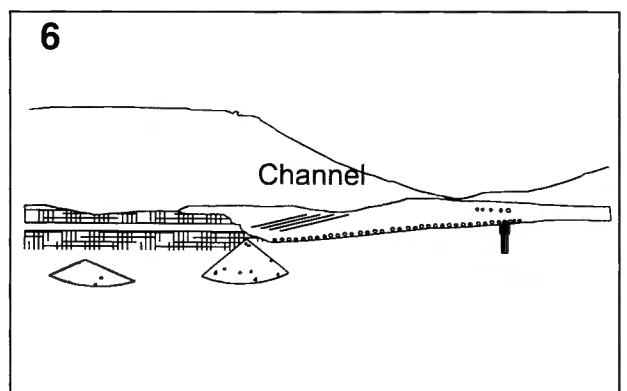
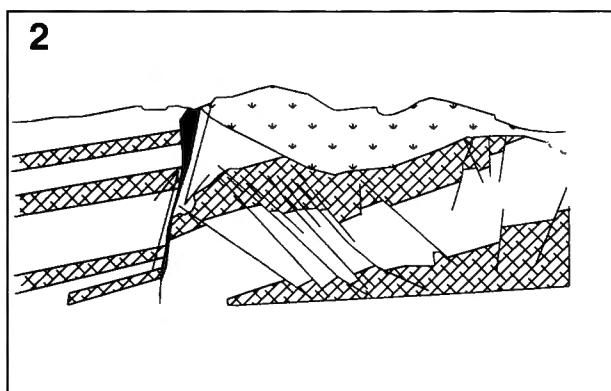
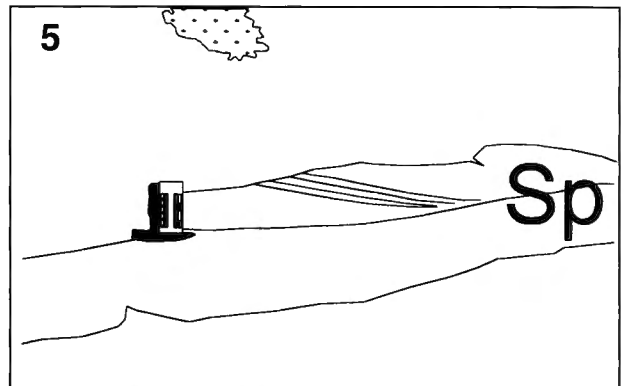
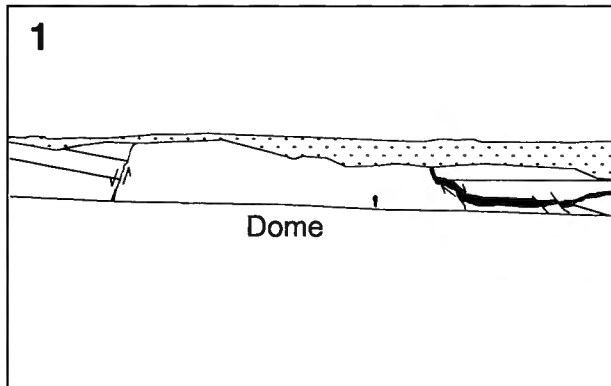
Thin sections of Bk horizon of the paleosols of the Lower Cretaceous of Dashuiguo (Inner Mongolia, P.R. China).

- Fig. 1 — Thin section of a calcareous nodule showing a fine micritic matrix with sparite filled cracks. (magnification 10×), within the matrix light and dark spots can be observed.  
 Fig. 2 — Detail of rhizolith with a concentric outline (magnification 100×).  
 Fig. 3 — Detail of a rhizolith recognized in the centre of the previous figure with the typical alveolar septal texture (magnification 100×).  
 Fig. 4 — Detail of a ped with a calcitic cutan (magnification 100×).  
 Fig. 5 — Detail of the centre of a satin spar vein. The dark line in the middle is the central parting from where the crystals grow outward (magnification 10×).  
 Fig. 6 — Detail of a satin spar vein showing the typical conoscopic form of the crystals (magnification 10×).  
 Fig. 7 — Thin section of the lithofacies P2 showing a poikilotopic texture and a brown coloring due to the presence of bacteria (magnification 10×).  
 Fig. 8 — Thin section of the lithofacies P2 showing a radial texture due tot the presence of *Microcodium* (magnification 10×).

## PLATE 4

Charophytes recovered from the Dashuiguo formation, Inner Mongolia (P.R. China). All specimens from sample DAH 99/30/80m (Fm2-lithofacies).

- Fig. 1 — *Porochara mundula* (PECK, 1941) 1a,b,c- lateral view (90×), illustrating the intraspecific variation. 1c represent the mean form of the species in lateral view. 1d- summit view (115×) with the large apical pore. 1e- basal view (115×).  
 Fig. 2 — *Aclistochara bransoni* (PECK, 1937) 2a- lateral view (90×). 2b- lateral view (80×). 2c- summit view (90×) with distinct apical depression. 2d- basal view (77.5×). 2e- deformed specimen (155×).  
 Fig. 3 — *Minhechara xiaoxiaoensis* YANG & ZHOU, 1983 3a- lateral view (115×). 3b- three quarter view of top and side (115×). 3c- summit view (115×). 3d- basal view (115×). 3e- detail of summit with distinct apical nodules (180×).  
 Fig. 4 — *Dasycladaceans* 4a- three quarter view of short specimen (85×). 4b- summit view of the same specimen (70×). 4c detail of the summit (280×). 4d- lateral view of long specimen (70×). 4e- three quarter view of the same specimen (70×).



P4087

col. 71 suppl.

01EC08X

- planches couleur (x4) entre p. 66 - 71

↓

recommander

